Supporting Information

Jastrab et al. 10.1073/pnas.1423319112

SI Experimental Procedures

Bacterial Strains, Growth Conditions, and Primers. *M. tuberculosis* strains were grown in Middlebrook 7H9 medium (Difco) supplemented with 0.2% glycerol, 0.05% Tween-80, 0.5% BSA, 0.2% dextrose, and 0.085% sodium chloride. Cultures were grown without shaking in 25-, 75-, or 125-cm^2 vented flasks (Corning Life Sciences) at 37 °C. For growth on solid medium, Middlebrook 7H11 agar (Difco) was supplemented with oleic acid, albumin, dextrose, and catalase (BBL). For selection using antibiotics, media were supplemented with 50 $\mu g \cdot mL^{-1}$ kanamycin, 50 $\mu g \cdot mL^{-1}$ hygromycin, and/or 25 $\mu g \cdot mL^{-1}$ streptomycin. *E. coli* cultures were grown in Luria–Bertani (LB) broth (Difco) at 37 °C, and LB agar was used as solid medium. For selection, media were supplemented with 100 $\mu g \cdot mL^{-1}$ kanamycin, 150 $\mu g \cdot mL^{-1}$ hygromycin, 50 $\mu g \cdot mL^{-1}$ streptomycin, or 200 $\mu g \cdot mL^{-1}$ ampicillin. Primers were purchased from Invitrogen, and plasmid sequencing was performed by GENEWIZ to confirm the veracity of cloned sequences.

Design and Expression of the Proteasome Trap Construct. Sewing overlap extension PCR was used to amplify the *prcBA* genes from *M. tuberculosis* chromosomal DNA. *prcB* was cloned without its N-terminal 57 codons to delete the N-terminal propeptide, to include a C-terminal FLAG-GGGG-His_6 tag, and, where indicated, to have its catalytic threonine mutated to Ala. These constructs were cloned along with the presumed native promoter region upstream of the *pup–prcBA* operon into the HindIII and XbaI sites of the mycobacterial overexpression vector pOLYG, and electroporated into *M. tuberculosis*. The production of stable protein was confirmed by immunoblotting.

TMT Labeling and MS Analysis. Protein was prepared as described in *Experimental Procedures*, resuspended in 6 M guanidine–HCl, and quantified by BCA protein assay (Thermo Scientific). Samples were reduced with 5 mM DTT, alkylated with 12 mM iodoacetamide, digested for 2 h with endoproteinase Lys-C (Wako) at a ratio of 1:200 LysC:protein, and then digested overnight with trypsin (Promega) at a ratio of 1:100 trypsin:protein. The digest was acidified with formic acid to a pH < 3, and peptides were desalted by using 50 mg of solid-phase C18 extraction cartridge (Waters) and then lyophilized. Samples were resuspended in 100 μL of 200 mM Hepes (pH 8.5) with 30% (vol/vol) acetonitrile, and 10 μL of 20 μg/mL 6-plex TMT reagent in anhydrous acetonitrile was added to each sample. The reaction proceeded for 1 h, and then was quenched with hydroxylamine to a final concentration of 0.5%. Samples were then combined equally, desalted by using homemade stage tips as described (1), and lyophilized.

After stage-tip desalting, samples were resuspended in 0.1% formic acid and analyzed on an Orbitrap Elite (Thermo Fisher Scientific) by using an Orbitrap LC-MS3 method as described (2). Spectra were matched against an *M. tuberculosis* H37Rv database (downloaded February 6, 2013), and protein false discovery rate was controlled to <1% by using the reverse-database strategy (3). Reporter ion S/N for all peptides matching each protein were summed, and protein relative expression values were represented as a fraction of the total intensity for all TMT reporter ions for the protein.

Purification of Recombinant Proteins. PafE was overproduced in *E. coli* BL21(DE3) or ER2566 at 37 °C from an isopropyl-B-D-1-thiogalactopyranoside (IPTG)-inducible plasmid encoding full-length PafE preceded by a His_6 affinity tag, and purified by Ni-NTA affinity purification as described in the QIAexpressionist manual (Qiagen). The fractions of interest were pooled, concentrated, and loaded onto either a HiLoad 16/600 Superdex 200 Prep Grade gel filtration column or a 10/300 Superose 6 GL gel filtration column (GE Healthcare Life Sciences) equilibrated with 10 mM Tris·HCl (pH 8.0), 50 mM NaCl, and 10% (vol/vol) glycerol. Fractions containing PafE were pooled and concentrated by using an Amicon Ultra-4 Centrifugal Filter Unit (Millipore). The final concentration of PafE was determined spectrophotometrically by using a Nanodrop (Thermo Scientific).

M. tuberculosis 20S CPs were purified from *E. coli* for microscopy and activity assays as follows: $20S_{OG}$ and $20S_{T1A}$ CPs were purified by using the described protocol (4). To produce WT 20S CPs, *prcBA* was cloned into the IPTG-inducible expression vector pET-32a(+) (Novagen) lacking the PrcB propeptide to circumvent the need for autoprocessing. This construct was introduced into the *E. coli* T7 expression strain ER2566, and expression was induced with 1 mM IPTG for 6 h at 37 °C. The bacteria were harvested by centrifugation, and the bacterial pellet was stored at −20 °C. Purification was otherwise performed as described (5).

M. tuberculosis HspR was purified as described (6, 7). Briefly, HspR was cloned into pET-32a(+) with a C-terminal His_6 tag, expression was induced with 1 mM IPTG for 5 h, and the protein was purified by Ni-NTA affinity chromatography under denaturing conditions by using 8 M urea. Fractions containing HspR were pooled, concentrated, and renatured by separation on a 10/300 Superose 6 GL gel-filtration column equilibrated with buffer containing 50 mM Tris (pH 7.5), 200 mM KCl, 5 mM EDTA, 5 mM $MgCl_2$, and 10% (vol/vol) glycerol. Desired fractions were pooled, concentrated, and frozen until use.

Negative Stain EM and Single Particle Image Processing. For negative staining of PafE, PafE–$20S_{OG}$ CP, and PafE–$20S_{T1A}$ CP samples, we first prepared carbon film substrate by evaporating a thin layer of carbon onto a piece of freshly cleaved mica in an Edwards vacuum evaporator (Sanborn) ($<10^{-5}$ Torr). We floated the mica on the surface of deionized water to peel off the carbon film and picked up film by 300-mesh copper EM grids. The carbon-coated grids were then glow discharged in a 100-mTorr argon atmosphere for 1 min. A 4- to 5-μL protein solution was applied to the EM grid for 1 min. Excess solution was removed by blotting the edge of the EM grid with a piece of filter paper, and the EM grid was then washed with ddH_2O, followed by staining twice for 30 s each in 5 μL of 2% (wt/vol) uranyl acetate aqueous solution. The EM grids were imaged in JEOL JEM-2010F transmission electron microscope operating at 200 kV. Micrographs were recorded in low-dose mode (15 $e^-/Å^2$) at ×50,000 microscope magnification in a Gatan UltraScan 4000 CCD camera (4,096 × 4,096 pixel), which corresponded to 2.12-Å/pixel sampling at the specimen level.

Particle selection and image processing were performed in an 8-CPU Dell Linux workstation by using EMAN (8) and EMAN2 (9) software packages. Raw particle images were selected in a semiautomatic manner with *e2boxer.py* in EMAN2. The selected particles were manually inspected to remove particles that were partially disassembled, having low contrast, and/or contacting other particles. The contrast transfer function was first determined with raw images and corrected for by flipping the phases. A second round of particle deletion was performed by computational *k*-means clustering classification. Phase-flipped raw particle datasets were then subjected to 2D classification.

Particles that belonged to the same classes were averaged to generate a set of high-contrast class averages. The number of particle images used for the final reference-free 2D classification was 17514, 229, 1969, 766 for PafE only, PafE–$20S_{T1A}$ purified from *M. tuberculosis*, PafE–$20S_{T1A}$ reconstituted by purified proteins, and PafE–$20S_{OG}$ with inhibitor, respectively.

Synthesis of LF-2 Peptide. The peptide sequence Lys-Lys-Val-Ala-Pro-Tyr-Pro-Met-Glu-Dpa(Dnp)–NH_2 was synthesized on resin by using a Syro II MultiSyntech Automated Peptide synthesizer (Biotage) using standard 9-fluorenylmethoxycarbonyl (Fmoc)-based solid-phase peptide chemistry at 25-μmol scale, using fourfold excess of amino acids in NMP relative to the resin. Benzotriazol-1-yl-oxytripyrrolidinophosphonium hexafluorophosphate (PyBOP, 4 equiv) and *N*,*N*-di-isopropylethylamine (8 equiv) were used as condensing reagents and all amino acids were introduced via double couplings (25 min each). Fmoc removal was carried out by using 20% (vol/vol) piperidine in *N*-methyl-2-pyrrolidone (NMP) for 2 × 2 and 1 × 5 min. The 7-methoxycoumarin-4-acetic acid (Mca) was introduced manually via double couplings (90 min each) by using *N*,*N*′-diisopropylcarbodiimide (4 equiv), *N*-hydroxybenzotriazole (4 equiv), and 4-dimethylaminopyridine (0.5 equiv) as condensing reagents. The product was simultaneously detached from the resin and deprotected by treatment with trifluoroacetic acid (TFA)/H_2O/triisopropyl silane [5 mL, 95:2.5:2.5 (vol/vol/vol)] for 3 h followed by precipitation with Et_2O/heptane [3:1 (vol/vol)]. The precipitate was washed 3× with Et_2O before it was dissolved in a mixture of H_2O/CH_3CN/HOAc [65:25:10 (vol/vol/vol)] and lyophilized. The crude product was purified on a Waters Auto-Purification preparative HPLC-MS system, equipped with a Waters Xbridge C18 column (130 Å, 5 μm, 19 × 150 mm), by using two mobile phases: A (0.05% TFA in water) and B (0.05% TFA in acetonitrile) at a flow rate of 30 mL/min; gradient: 0–2.5 min, 18% B; 2.5–17.5 min, →48% B; 17.5–19.5 min, →95% B, 19.5–20.9 min 95% B, 20.9–21.0 min →5% B. The product was obtained as a yellow powder (7 mg, 18%) and was analyzed by LC-MS on a system equipped with a Waters 2795 Separation Module (Alliance HT), Waters 2996 Photodiode Array Detector (190–750 nm), Phenomenex Kinetex C18 (2.1 × 100, 2.6 μm) and LCTTM Orthogonal Acceleration Time of Flight Mass Spectrometer by using two mobile phases: buffer A [0.1% formic acid in H_2O/acetonitrile 99:1 (vol/vol)] and B [0.1% formic acid in H_2O/acetonitrile 99:1 (vol/vol)] at a flow rate of 400 μL/min; gradient: 0–0.5 min, 5% B; 0.5–8 min, →95% B; 8–10 min 95% B, 10–12 min, →5% B. R_t: 4.48 min; MS ES+ (amu) calculated for $C_{70}H_{96}N_{16}O_{21}S$: 1,529.67 $[M+H]^+$, found: 1,529.4 $[M+H]^+$, 764.9 $[M+2H]^{2+}$, 510.7 $[M+3H]^{3+}$.

Solvents were purchased from BIOSOLVE, peptide synthesis reagents were purchased from Novabiochem, except for Fmoc-PAL-PEG-PS resin (0.2 mmol/g), which was purchased from Rapp Polymere GmbH, and Mca and Fmoc-L-Dpa(Dnp)-OH, which were obtained from Chem-Impex. The following protected amino acid building blocks were used during the peptide synthesis: Fmoc-L-Ala-OH, Fmoc-L-Dpa(Dnp), Fmoc-L-Glu(OtBu)-OH, Fmoc-Lys(Boc)-OH, Fmoc-L-Met-OH, Fmoc-L-Pro-OH, Fmoc-L-Tyr(tBu)-OH, Fmoc-L-Val-OH.

Production of Pup∼PanB–Fluorescein. The *panB* gene from *M. tuberculosis* was cloned into a pET3a vector (EMD Millipore) between NdeI and BamHI sites with a C-terminal His_6 tag, and the plasmid was used to transform *E. coli* BL21(DE3). PanB–His_6 was purified by Ni-NTA affinity chromatography as described in the QIAexpressionist manual (Qiagen), and further purified by SEC using a 10/300 GL Superdex 200 column (GE Healthcare). Fractions containing pure PanB were identified by 15% (wt/vol) SDS/PAGE and quantified by comparison with Coomassie Brilliant Blue-stained BSA standards.

A total of 80 μL of 755 μM PanB was exchanged into buffer consisting of 20 mM NaP, 150 mM NaCl, and 5 mM EDTA at pH 7.5 by using a protein-desalting spin column (Thermo Scientific). The resulting PanB solution was incubated with 1.0 mg of fluorescein-5-maleimide (Thermo Scientific) at 4 °C overnight to facilitate specific labeling of cysteine residues. Excess fluorescein was removed by desalting three times through spin columns, yielding 100 μL of 100 μM PanB-fluorescein.

The PanB–fluorescein conjugate was subjected to pupylation with 200 μM *M. tuberculosis* His_6-PupE and 1 μM PafA in Buffer P [50 mM Tris·HCl, 300 mM NaCl, 20 mM MgCl2, 5 mM ATP, 1 mM DTT, and 10% (vol/vol) glycerol at pH 7.4] in a final volume of 100 μL. The pupylation reaction was allowed to proceed overnight at 37 °C to push pupylation to completion. The overnight reaction was stopped by applying the assay mixture to a spin column pre-equilibrated in PBS at pH 7.5. Under these conditions, the small amount of PafA present aggregated on the column, effectively removing it from the assay products. His_6–PupE was also retained on the column due to its small size (∼7.7 kDa), and the desired Pup∼PanB–fluorescein conjugate was recovered in the eluate. Pup∼PanB–fluorescein was further purified by SEC using a 10/300 GL Superdex 200 column pre-equilibrated in buffer P. Fractions containing >90% pure Pup∼PanB–fluorescein were identified by 15% (wt/vol) SDS/PAGE, combined, and used for proteolysis assays.

1. Rappsilber J, Ishihama Y, Mann M (2003) Stop and go extraction tips for matrix-assisted laser desorption/ionization, nanoelectrospray, and LC/MS sample pretreatment in proteomics. *Anal Chem* 75(3):663–670.
2. McAlister GC, et al. (2012) Increasing the multiplexing capacity of TMTs using reporter ion isotopologues with isobaric masses. *Anal Chem* 84(17):7469–7478.
3. Elias JE, Gygi SP (2007) Target-decoy search strategy for increased confidence in large-scale protein identifications by mass spectrometry. *Nat Methods* 4(3):207–214.
4. Li D, et al. (2010) Structural basis for the assembly and gate closure mechanisms of the Mycobacterium tuberculosis 20S proteasome. *EMBO J* 29(12):2037–2047.
5. Lin G, et al. (2006) Mycobacterium tuberculosis prcBA genes encode a gated proteasome with broad oligopeptide specificity. *Mol Microbiol* 59(5):1405–1416.
6. Bandyopadhyay B, Das Gupta T, Roy D, Das Gupta SK (2012) DnaK dependence of the mycobacterial stress-responsive regulator HspR is mediated through its hydrophobic C-terminal tail. *J Bacteriol* 194(17):4688–4697.
7. Das Gupta T, Bandyopadhyay B, Das Gupta SK (2008) Modulation of DNA-binding activity of Mycobacterium tuberculosis HspR by chaperones. *Microbiology* 154(Pt 2): 484–490.
8. Ludtke SJ, Baldwin PR, Chiu W (1999) EMAN: Semiautomated software for high-resolution single-particle reconstructions. *J Struct Biol* 128(1):82–97.
9. Tang G, et al. (2007) EMAN2: An extensible image processing suite for electron microscopy. *J Struct Biol* 157(1):38–46.

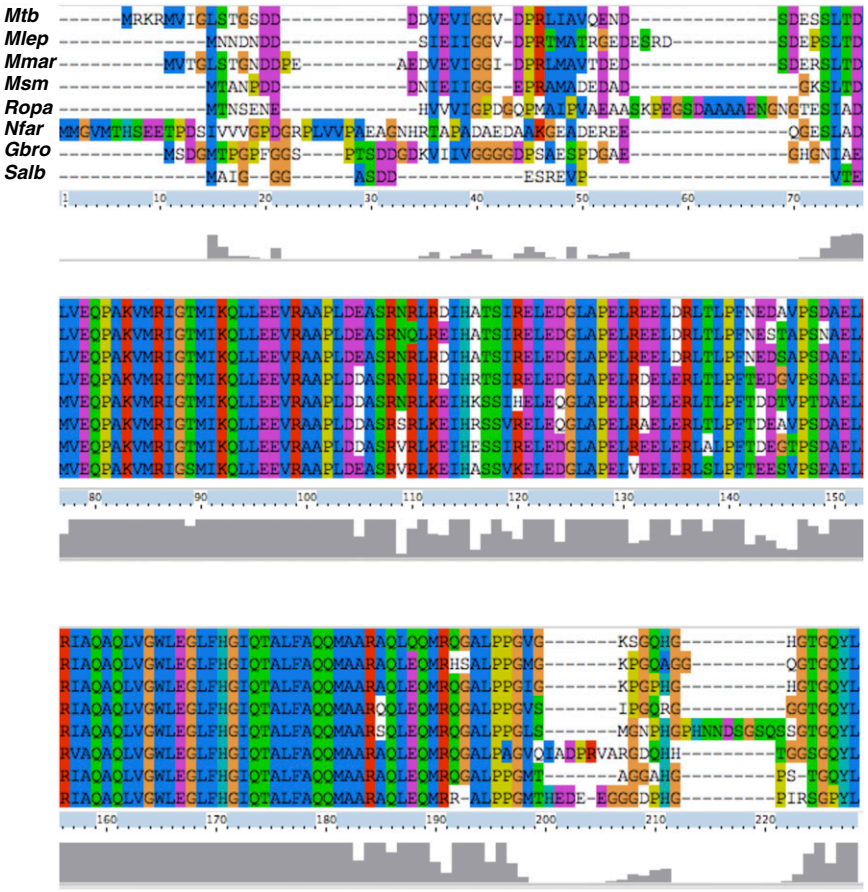

Fig. S1. Primary structure of PafE. Alignment of the PafE amino acid sequence from *M. tuberculosis* (*Mtb*), *Mycobacterium leprae* (*Mlep*), *Mycobacterium marinum* (*Mmar*), *Mycobacterium smegmatis* (*Msm*), *Rhodococcus opacus* (*Ropa*), *Nocardia farcinica* (*Nfar*), *Gordonia bronchialis* (*Gbro*), and *Streptomyces* alboviridis (*Salb*). Alignment was performed by using ClustalX.

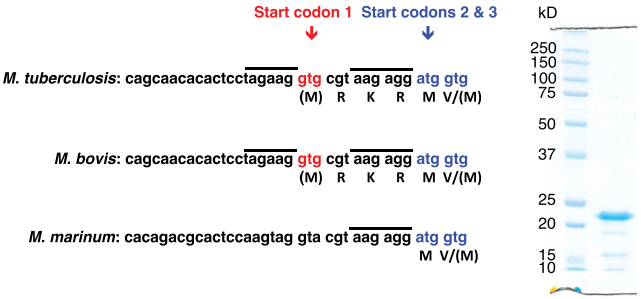

Fig. S2. *pafE* has three potential translational start sites. (*Left*) Alignment of the 5′ regions of *pafE* from different mycobacterial species. Horizontal lines indicate putative ribosome binding sites. (*Right*) PafE was produced in *E. coli* with an N-terminal thrombin-cleavable His_6 tag, purified by subsequent rounds of Ni-NTA and SEC, separated by 12% (wt/vol) SDS/PAGE, and visualized by Coomassie Brilliant Blue staining.

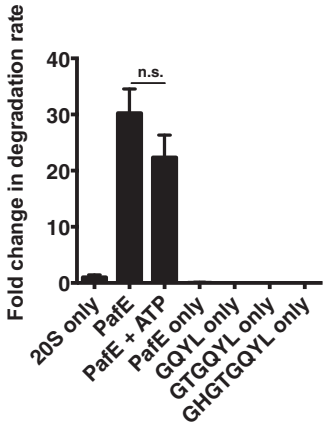

Fig. S3. PafE-mediated proteasome activation is ATP-independent. LF-2 degradation assays were performed as described in the main text, except that 5 mM ATP was included where indicated. Statistical analysis was performed by using Student's *t* test. n.s., not significant.

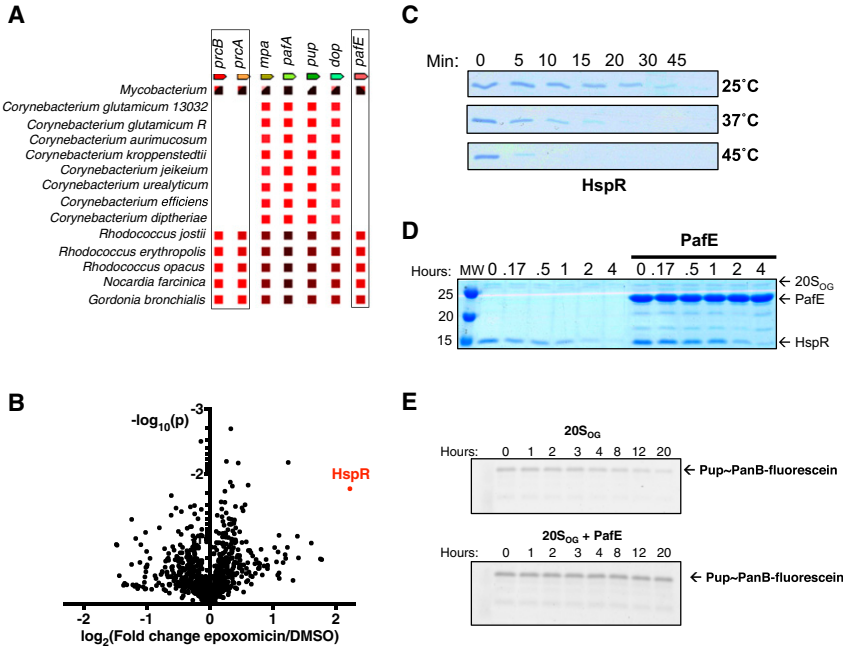

Fig. S4. HspR is a PafE-dependent and pupylation-independent proteasome substrate. (*A*) STRING-DB analysis of proteasome and pupylation system genes in actinobacteria. Squares denote the presence of a homolog of the indicated gene. Darker color indicates a higher level of homology with *M. tuberculosis* strain H37Rv. (*B*) Proteomic identification of putative pupylation-independent proteasome substrates in *M. tuberculosis*. Protein lysates were prepared from WT and *pafA* strains grown to $OD_{580} \sim 0.75$ and treated with 50 μM epoxomicin for 4 d. Lysates were prepared and analyzed similarly by TMT-MS. The $\log_2$ ratio of abundance in epoxomicin-treated vs. DMSO-treated cultures was plotted against the $\log_{10}$ *P* value as determined by *t* test using three biological replicates. The data point representing HspR is in red. (*C*) HspR degradation rate increases at high temperatures. HspR degradation assay was performed as in Fig. 6*D* except with incubation at the indicated temperatures. (*D*) In vitro degradation of HspR–His_6 was performed as in Fig. 6*D*, except $20S_{OG}$ CP–His_6 was used with and without His_6–PafE. The contrast was adjusted to better visualize the $20S_{OG}$ CP–His_6. (*E*) Open-gate 20S CPs do not degrade the Mpa-dependent proteasome substrate Pup~PanB. Recombinant purified $20S_{OG}$ CP, Pup~PanB–fluorescein, and where indicated PafE were mixed and incubated at room temperature. Aliquots were removed at the indicated time points and separated by 12% (wt/vol) SDS/PAGE, and Pup~PanB–FITC degradation was monitored by in-gel fluorescence.

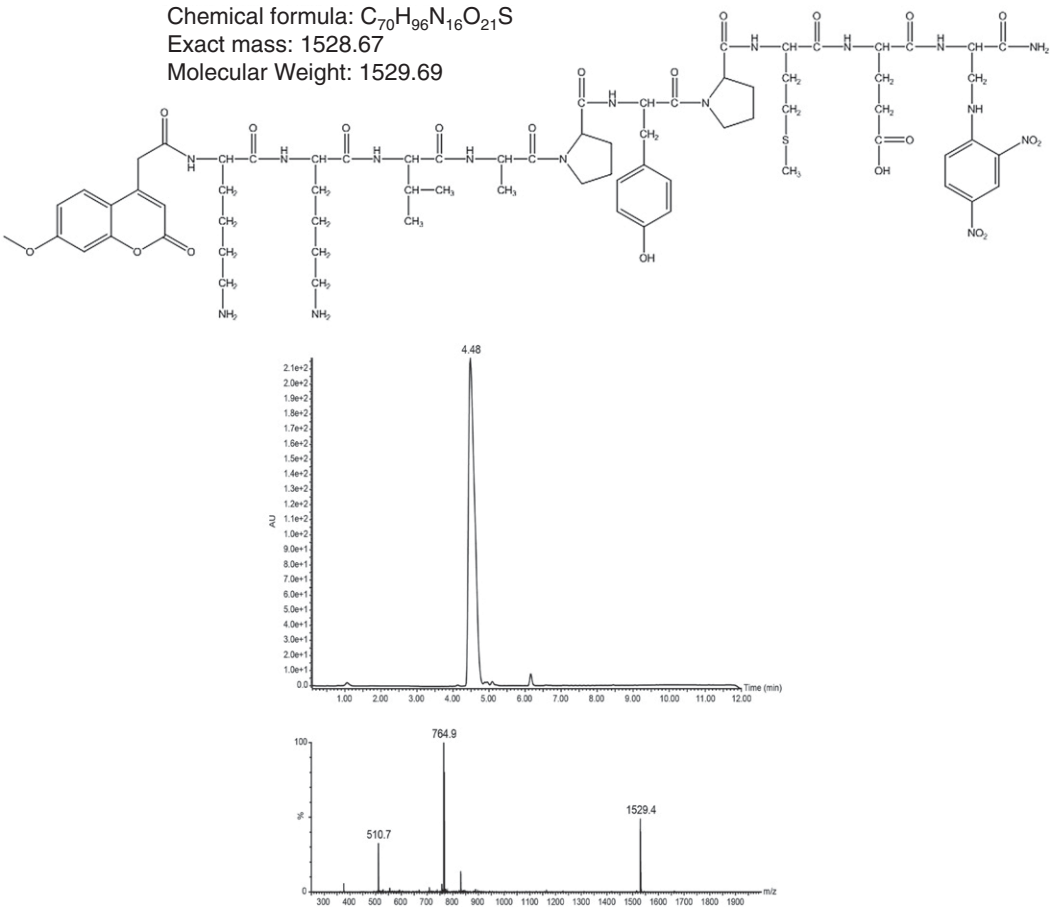

Fig. S5. Chemical structure (*Upper*) and LC-MS analysis (*Lower*) of LF-2 peptide [Mca KKVAPYPME-Dpa(Dnp)-amide].

Table S1. Proteins copurifying with the 20S CP from WT *M. tuberculosis*. Data are organized from highest to lowest abundance found in Trap purifications. Column labeled protein: Rv number of each protein identified. Column labeled peptides: the number of unique peptides identified for a given protein. Columns labeled WT and Trap 1–3: relative abundance of each protein that purified with WT or Trap proteasomes in each biological replicate; related to Fig. 1*B*, *Left*

Table S1

Table S2. Proteins copurifying with the 20S CP from an *M. tuberculosis mpa* mutant. Data are organized from highest to lowest abundance found in Trap purifications. Column labeled protein: Rv number of each protein identified. Column labeled peptides: the number of unique peptides identified for a given protein. Columns labeled WT and Trap 1–3: relative abundance of each protein that purified with WT or Trap proteasomes in each biological replicate; related to Fig. 1*B*, *Right*

Table S2

Table S3. Proteins that accumulated in *pafE* mutant vs. parental *M. tuberculosis* strains. Data are organized from highest to lowest fold change. Column labeled protein: Rv number of each protein identified. Column labeled peptides: the number of unique peptides identified for a given protein. Columns labeled parental and *pafE* 1–3: relative abundance of each protein found in parental or *pafE* lysates for each biological replicate; related to Fig. 6*C*, *Left*

Table S3

Table S4. Proteins that accumulated in an *M. tuberculosis pafA* mutant treated with epoxomicin vs. DMSO. Data are organized from highest to lowest fold change. Column labeled protein: Rv number of each protein identified. Column labeled peptides: the number of unique peptides identified for a given protein. Columns labeled DMSO and epoxomicin 1–3: relative abundance of each protein found in DMSO or epoxomicin-treated bacteria for each biological replicate; related to Fig. 6*C*, *Right*

Table S4

Table S5. Bacterial strains, plasmids, and primers

Table S5

1. Chong YH, et al. (1994) Bacterial expression, purification of full length and carboxyl terminal fragment of Alzheimer amyloid precursor protein and their proteolytic processing by thrombin. *Life Sci* 54(17):1259–1268.
2. Darwin KH, Ehrt S, Gutierrez-Ramos JC, Weich N, Nathan CF (2003) The proteasome of Mycobacterium tuberculosis is required for resistance to nitric oxide. *Science* 302(5652):1963–1966.
3. Gandotra S, Lebron MB, Ehrt S (2010) The Mycobacterium tuberculosis proteasome active site threonine is essential for persistence yet dispensable for replication and resistance to nitric oxide. *PLoS Pathog* 6(8):e1001040.
4. Garbe TR, et al. (1994) Transformation of mycobacterial species using hygromycin resistance as selectable marker. *Microbiology* 140(Pt 1):133–138.
5. Stover CK, et al. (1991) New use of BCG for recombinant vaccines. *Nature* 351(6326):456–460.
6. Bardarov S, et al. (2002) Specialized transduction: An efficient method for generating marked and unmarked targeted gene disruptions in Mycobacterium tuberculosis, M. bovis BCG and M. smegmatis. *Microbiology* 148(Pt 10):3007–3017.